Supporting Information

Endoplasmic Reticulum-Targeted Ratiometric NHC-Borane Probe for Two-Photon Microscopic Imaging of Hypochlorous Acid

Yen Leng Pak[‡a], Sang Jun Park[‡b], Gyeongok Song[c], Yubin Yim[a], Hyuk Kang[c], Hwan Myung Kim*[b,c], Jean Bouffard*[a], and Juyoung Yoon*[a].

[a]Department of Chemistry and Nano Science (BK 21 Plus), Ewha Womans University, Seoul 03760, Korea

[b]Department of Energy Systems Research, Ajou University, Suwon, Gyeonggi-do 443-749, Korea.

[c]Department of Chemistry, Ajou University, Suwon, Gyeonggi-do 443-749, Korea.

* E-mail: kimhm@ajou.ac.kr. Phone: +82 (031) 219-2609

* E-mail: bouffard@ewha.ac.kr. Phone: +82 (02) 3277-3427

* E-mail: jyoon@ewha.ac.kr. Phone: +82 (02) 3277-2400

Table of Content

1. Synthetic Procedures.

Compounds 1 and 2

Compounds **1**[S1] and **2**[S2,S3] were prepared according to published procedures.

Synthesis of 3

2 (1 g, 5.52 mmol) and CH_3I (3.1 mL, 2.20 mmol) in CH_3CN (15 mL) were stirred under reflux for 12 h. After cooling to room temperature, the solvents were removed under vacuum, and the residue was purified by silica gel column chromatography, using CH_2Cl_2/CH_3OH (20/1, v/v) as eluent to yield **3** a white solid (0.95 g, 4.82 mmol, 87 %). ^{1}H NMR (DMSO-d_6, 300 MHz) δ (ppm): 9.83 (br, s, 1H), 8.61 (s, 2H), 8.25-8.20 (m, 2H), 7.71-7.66 (m, 2H), 4.16 (s, 6H). ^{13}C NMR (DMSO-$_{d6}$, 75 MHz) δ (ppm): 147.9, 131.6, 131.6, 128.9, 127.3, 111.4, 34.0 HR-MS (ESI) m/z calcd. for $C_{13}H_{13}N_2^+$ $[M]^+$ = 197.1073, found: 197.1096.

2. Experimental procedures

Determination of the Fluorescence Quantum Yield. The quantum yield of the probe was determined according to following equation:

$$\Phi_x = \Phi_s \times (D_x/D_s) \times (A_s/A_x) \times (\eta_x/\eta_s)^2$$

where Φ_s is the quantum yield of the standard, D is the area under the emission spectra, A is the absorbance at the excitation wavelength, and η is the refractive index of the solvent used. x subscript denotes unknown, and s means standard. We chose Quinine sulfate (Φ = 0.54 in 0.1 M of H_2SO_4, refractive index, n = 1.33) as the standard.[S4]

Density functional theory (DFT) calculation. Time-dependent density functional theory (TD-DFT) calculations were performed with the Gaussian 09 program package.[S5] Ground state geometry was optimized at B3LYP/6-311++G level of theory, and excited state geometry was optimized at TD-B3LYP/6-311++G level of theory. Vertical transition energy at each geometry, which corresponds to absorption and emission maximum wavelength respectively, was calculated TD-B3LYP/6-311++G level of theory.

Two-Photon Fluorescence Microscopy. Two-photon fluorescence microscopy images of **4** were obtained with multiphoton microscopes (Leica TCS SP8 MP) with ×40 oil objectives. Probe was excited 720 nm by a mode-locked titanium-sapphire laser source (Mai Tai HP) with an output power of 1.98 W, which corresponded to approximately 9.19×10^5 W cm^{-2} average power in the focal plane.

Cell Culture. The cells were cultured on glass bottomed dishes (NEST) for 2 days under a 5 % CO_2 humidified atmosphere at 37 °C and. For imaging, the growth medium was replaced with serum-free medium, treated with **4** (10 μM) and incubated for 30 min. The culture medium is DMEM (WelGene) supplemented with 10 % FBS, streptomycin (100 μg mL^{-1}) and penicillin (100 units mL^{-1}).

Photostability. Photostability of **4** in Raw 264.7 cells was determined by monitoring the changes in TPEF intensity with time at three designated positions of **4** labeled cells. The digitized intensity was recorded with 2.00 sec intervals for the duration of 1 h using *xyt* mode. The TPEF intensities were collected at 380-600 nm upon excitation at 720 nm with femto-second pulses.

Co-localization Experiment. Co-localization experiments were performed by co-staining with Raw 264.7 cells in the appropriate combinations of 10 μM of **4** and each commercial organelle tracker (1.0 μM) for 30 min. Excitation wavelengths for TPM and OPM are 720 nm and 552 nm, respectively, and the corresponding emissions were collected at 380−550 nm (**4**) and 600−650 nm (organelle trackers). The Pearson's colocalization coefficient (*A*) was calculated using the AutoQuant X2 program.

Preparation and Imaging of Rat Hippocampus. Slices were prepared from the hippocampi of 14 days old male SD rat and cut into 400 μm thickness using a vibrating-blade microtome in DPBS (Gibco). Slices were incubated with **4** (100 μM, 1.5 h) under a 5% CO_2, 37 °C atmosphere for 1 h. Slices were then washed two times with DPBS and taken to glass-bottomed dishes. The TPM images were acquired at about 70−190 μm depth.

Determination of Octanol-PBS Partition Coefficient (log P_{oct}). 20 μL of **4** solution in DMSO (20 mM) was added to 5 mL *n*-octanol. Then, this solution was added 5 mL of PBS buffer (10 mM PBS, pH 7.4). The resulting mixture was stirred in the dark for 10 min. The probe concentration in each layer was measured spectrophotometrically, using their molar extinction coefficients shown in Table S1. The log P_{oct} value was calculated by using $\log P_{oct} = \log [\text{Probe}]_{oct} - \log [\text{Probe}]_{PBS}$; where the $[\text{Probe}]_{oct}$ and $[\text{Probe}]_{PBS}$ are the concentrations of the probe in *n*-octanol and PBS, respectively.

Cell viability. Cells were seeded in a 96-well plate with culture media. After 24 hr culture, cells were incubated with probe **4** for 24 hr and washed with DPBS. To identify cell viability, 0.5 mg/ml of MTT (Sigma) media was added to the cells for 4 hr, and the produced formazan was dissolved in 0.1 ml of dimethylsulfoxide (DMSO) and read at OD 650 nm with a Spectramax Microwell plate reader.

3. Spectroscopic Properties and Fluorescence Assays in Solution.

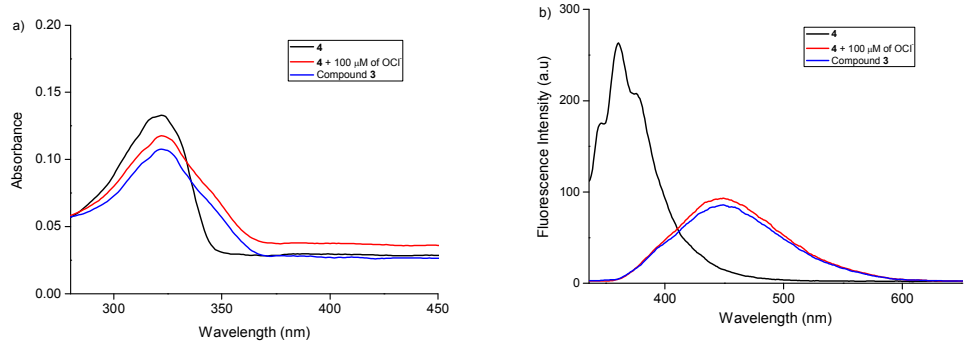

Figure S1. UV-vis (a) and fluorescence (b) spectra of probe **4** (10 μM) before and after the addition of OCl^- (100 μM), superimposed with the spectra of compound **3**.

Table S1. Lowest transition wavelength of **3** and **4**.

Molecule	Absorption maximum (nm)	Oscillator strength at ground state geometry	Emission maximum (nm)	Oscillator strength at excited state geometry
3	384.04	0.0435	466.29	0.0357
4	313.67	0.0704	347.37	0.0759

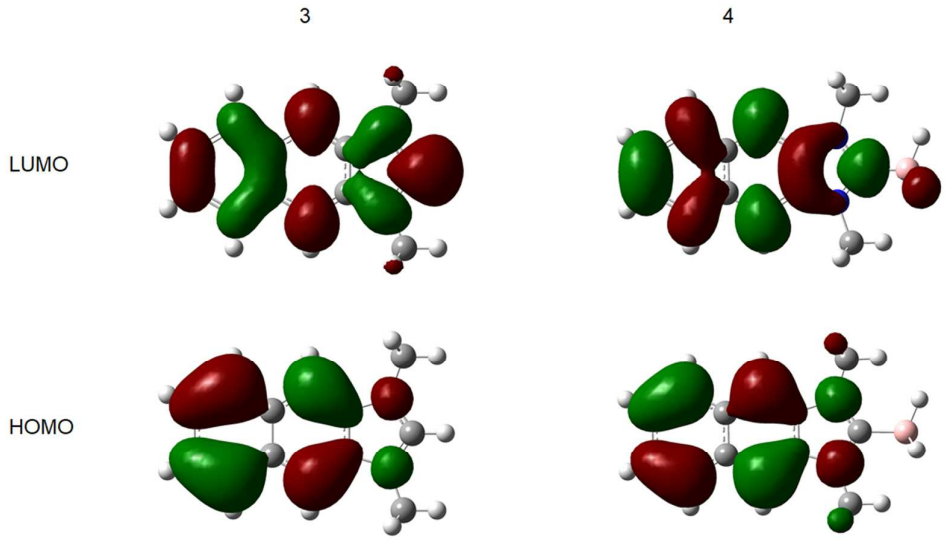

Figure S2. Highest occupied molecular orbital (HOMO) and lowest unoccupied molecular orbital (LUMO) of **3** and **4**.

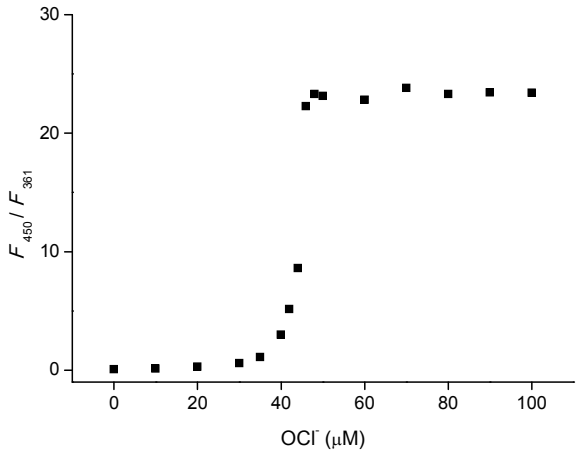

Figure S3. Ratiometric calibration curve of the **4** probe in the presence of OCl^-, plotting the fluorescence intensity ratio (F_{450}/F_{361}) against the OCl^- concentration (λ_{ex} = 326 nm; RT, 10:90 CH_3CN-Aq. PBS, 10 mM, pH 7.4).

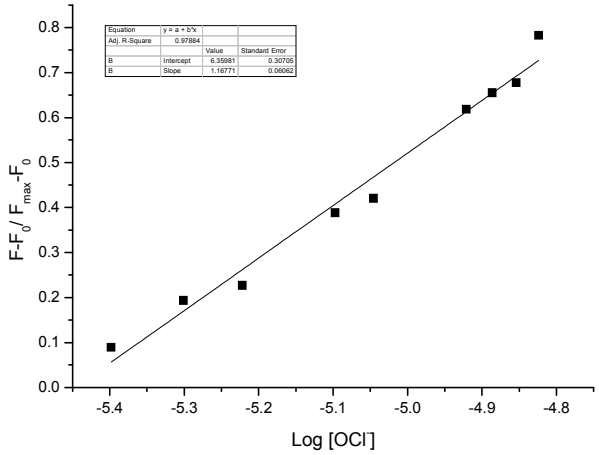

Figure S4. Calculation of the OCl^- detection limit of probe **4** (1 μM; F = I_{361}). The detection limit was taken as concentration corresponding to the Y-axis intercept of the linear regression, where log[OCl^-] = -5.446, or [OCl^-] = 3.6 μM.

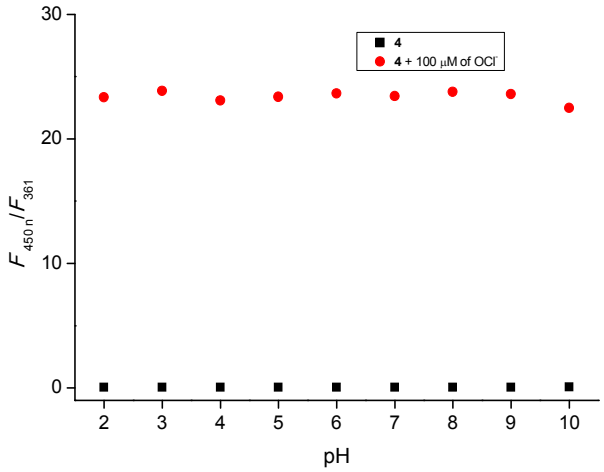

Figure S5. pH effect on fluorescence intensity ratio of **4** (10 μM) in the absence and presence of OCl^- (100 μM) with excitation at 326 nm.

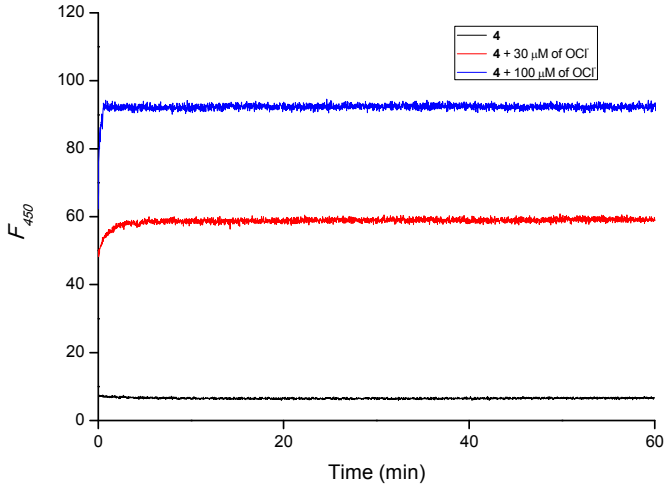

Figure S6. Time courses of **4** intensity at 450 nm (10 μM) in the absence and presence of OCl^- (30 μM and 100 μM) with excitation at 326 nm.

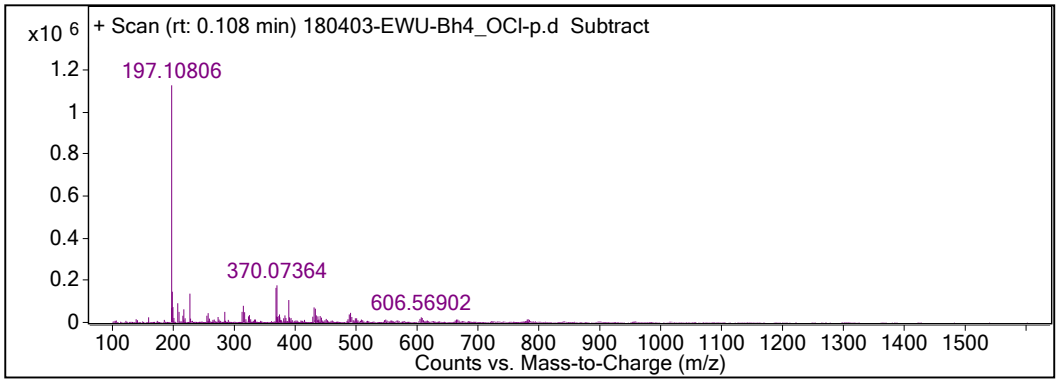

Figure S7. ESI-MS spectrum after the reaction of **B4** (10 μM) with OCl^- (100 μM).

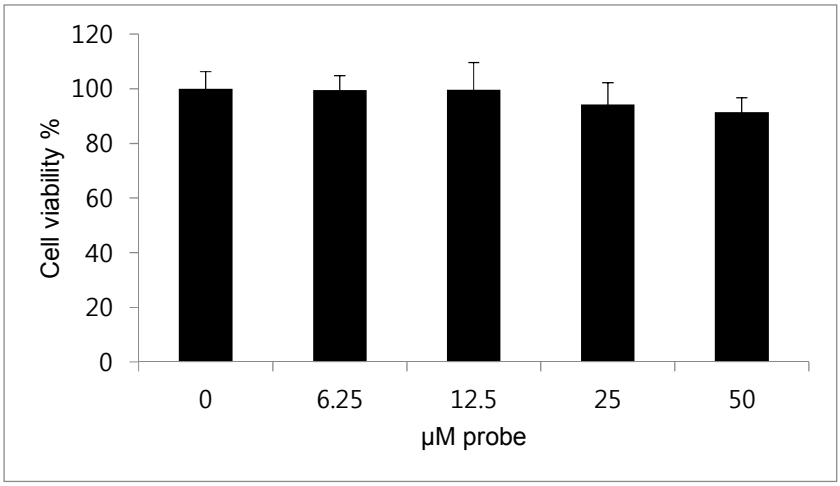

Figure S8. Cytotoxicity of probe **4**.

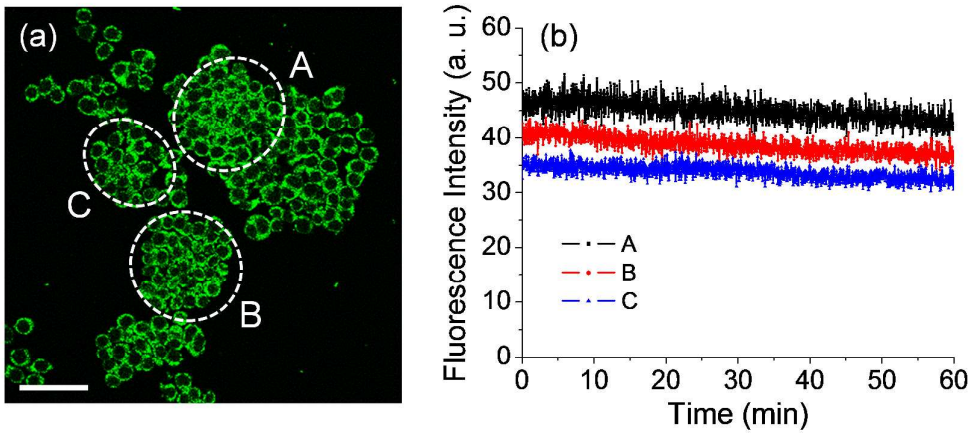

Figure S9. (a) TPM image of **4** in Raw 264.7 cells and (b) corresponding relative fluorescence intensity from A-C. Fluorescence intensity was recorded for 1 h with 2 sec intervals. The TPM image was acquired at 380-600 nm upon excitation at 720 nm. Scale bar = 50 μm.

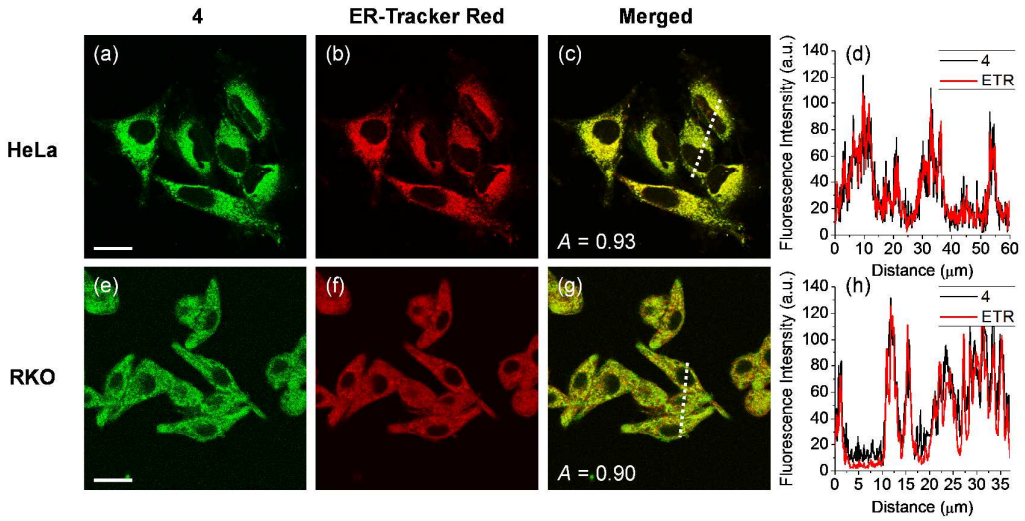

Figure S10. (a and e) TPM and (b and f) OPM images of (a–c) HeLa and (e–g) RKO cells co-labeled with **4** (10 μM) and ER-Trackers Red (1.0 μM). (c and g) Merged images. (d and h) Line profile of fluorescence intensity obtained from corresponding cells images. Excitation wavelengths for TPM and OPM are 720 nm and 552 nm, respectively, and the corresponding emissions were collected at 380−550 nm (**4**) and 600−650 nm (ER-Tracker Red). Scale bars = (a) 25 and (e) 20 μm.

Table S2. Molar extinction coefficient and log P_{oct} for **4** in *n*-octanol and PBS buffer.

Probe	Solvent	ε (10^{-4} M^{-1} cm^{-1})	log P_{oct}
4	*n*-octanol	1.38	1.04 ± 0.02
	PBS	0.71	

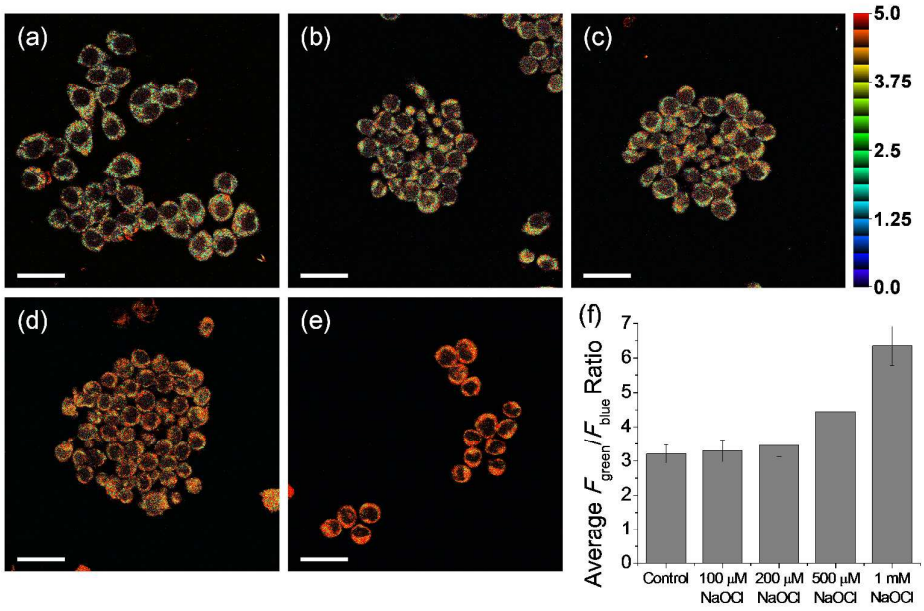

Figure S11. Pseudocolored ratiometric TPM images of Raw 264.7 cells labeled with **4** (10 μM) for 30 min. (a) Control image. (b–e) Cells pretreated with NaOCl for 100 μM, 200 μM, 500 μM and 1 mM for 30 min respectively and then incubated with **4**. **(**f) Average F_{green}/F_{blue} ratios in the TPM images. Excitation wavelength for **4** is 720 nm and TPM images were obtained at 380−430 nm (blue) and 450−600 nm (green). Scale bars = 20 μm.

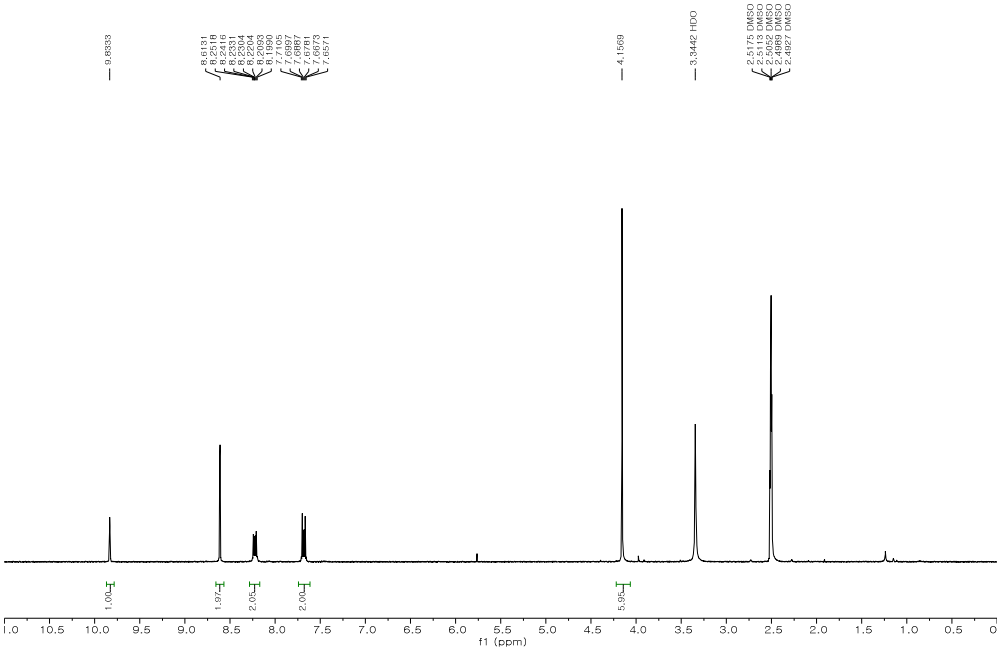

Figure S12. ^{1}H NMR of **3**.

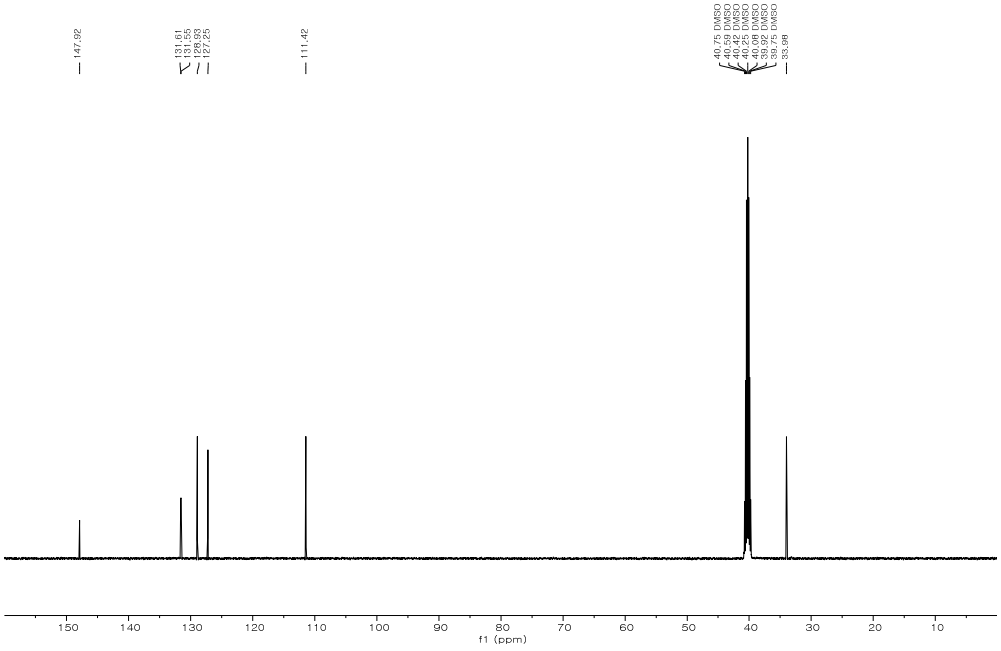

Figure S13. ^{13}C NMR of **3**.

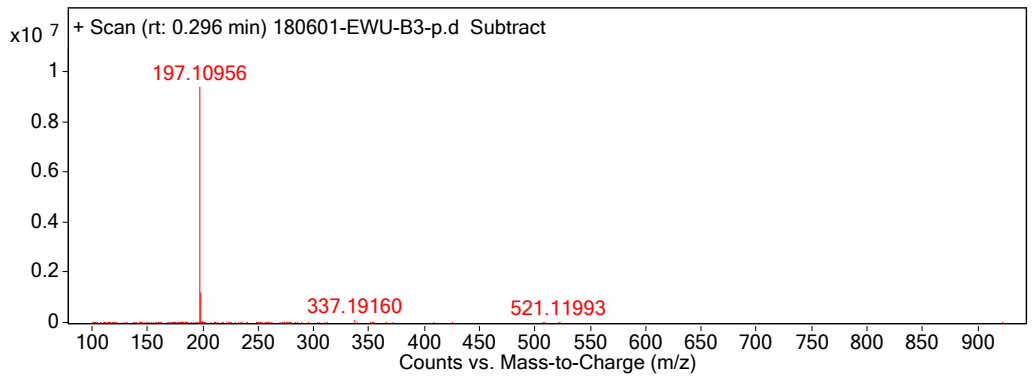

Figure S14. ESI mass spectrum of **3**.

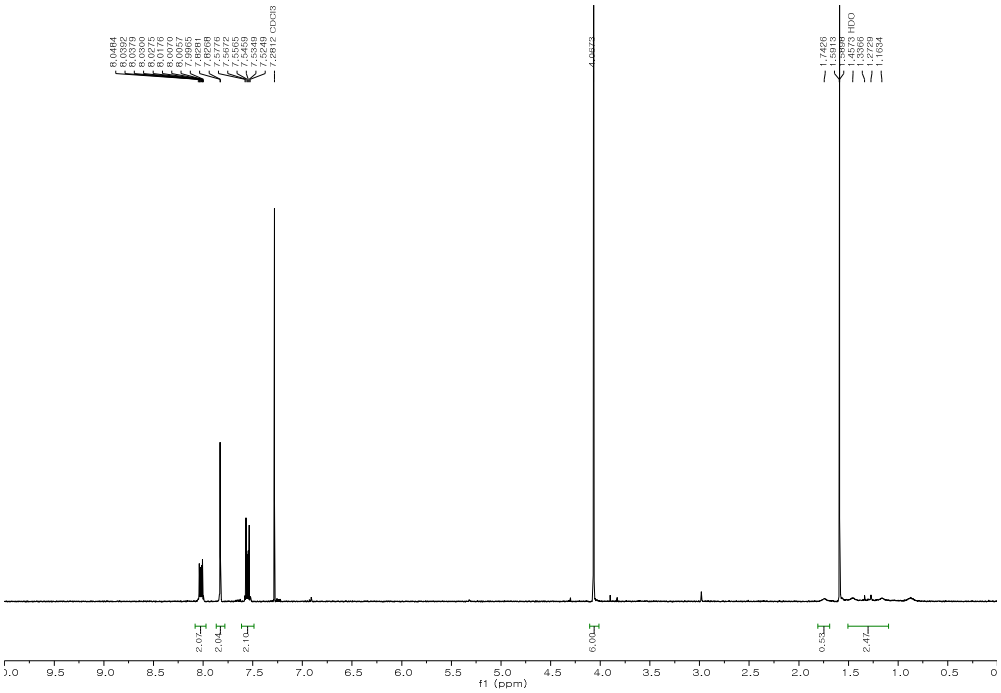

Figure S15. ^{1}H NMR of **4**

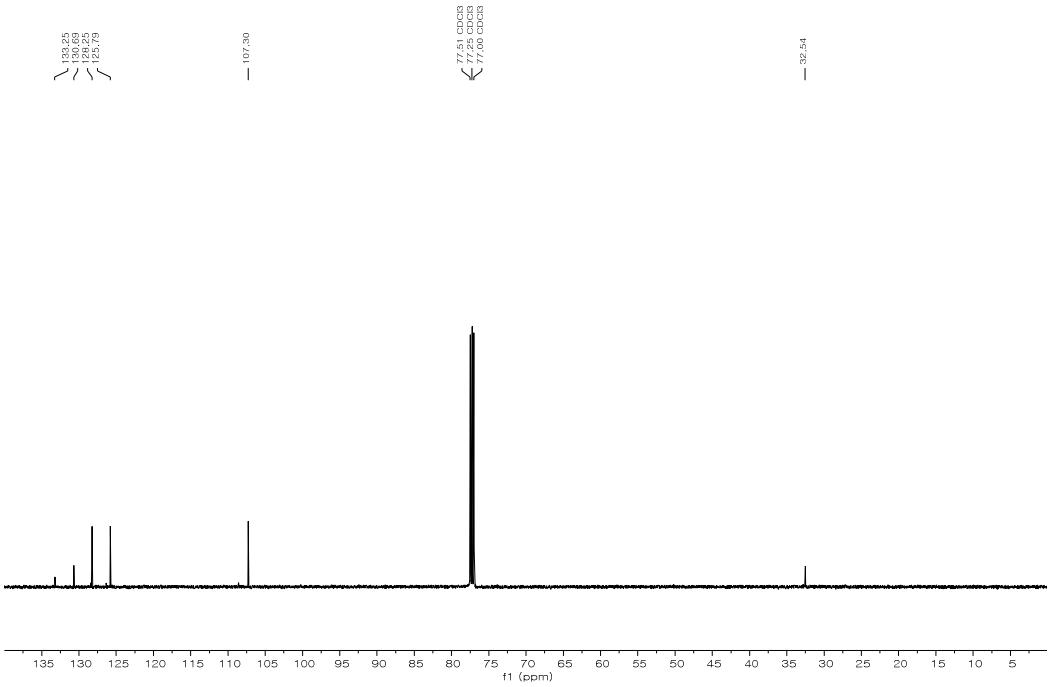

Figure S16. ^{13}C NMR of **4**

.

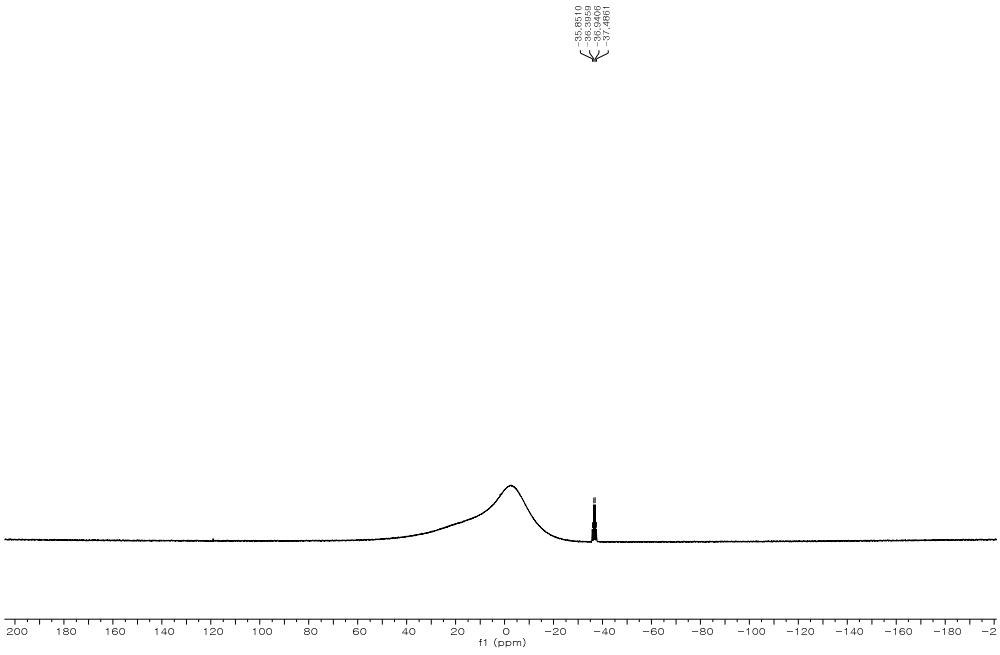

Figure S17. ^{11}B NMR of **4**

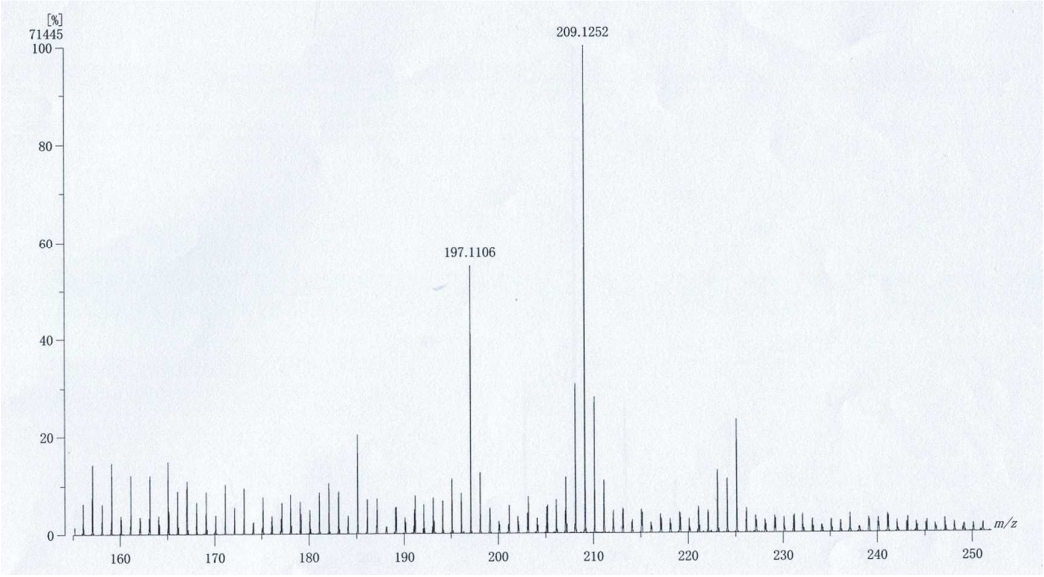

Figure S18. FAB spectrum of **4**.

References

S1. Grobler, I.; Smith, V. J.; Bhatt, P. M.; Herbert, S. A.; Barbour, L. Tunable Anisotropic Thermal Expansion of a Porous Zinc(II) Metal–Organic Framework. *J. Am. Chem. Soc.* **2013**, *135*, 6411-6414.

S2. Xu, Z.; Kim, S. K.; Han, S. J.; Lee, C.; Kociok-Kohn, G.; James, T. D.; Yoon, J. Ratiometric Fluorescence Sensing of Fluoride Ions by an Asymmetric Bidentate Receptor Containing a Boronic Acid and Imidazolium Group. *Eur. J. Org. Chem*. **2009**, 3058-3065.

S3. Lee, M.; Moon, J. H.; Jun, E. J. Kim, G.; Kwon, Y.; Lee, J. Y.; Yoon, J. A tetranaphthoimidazolium receptor as a fluorescent chemosensor for phytate. *Chem. Commun*. **2014**, *50*, 5851-5853.

S4. Melhuish, W. H. QUANTUM EFFICIENCIES OF FLUORESCENCE OF ORGANIC SUBSTANCES: EFFECT OF SOLVENT AND CONCENTRATION OF THE FLUORESCENT SOLUTE[1]. *J. Phys. Chem.* **1961**, *65*, 229-235.

S5. Gaussian 09, Revision C.01, Frisch, M. J.; Trucks, G. W.; Schlegel, H. B.; Scuseria, G. E.; Robb, M. A.; Cheeseman, J. R.; Scalmani, G.; Barone, V.; Mennucci, B.; Petersson, G. A.; Nakatsuji, H.; Caricato, M.; Li, X.; Hratchian, H. P.; Izmaylov, A. F.; Bloino, J.; Zheng, G.; Sonnenberg, J. L.; Hada, M.; Ehara, M.; Toyota, K.; Fukuda, R.; Hasegawa, J.; Ishida, M.; Nakajima, T.; Honda, Y.; Kitao, O.; Nakai, H.; Vreven, T.; Montgomery, J. A.; Jr.; Peralta, J. E.; Ogliaro, F.; Bearpark, M.; Heyd, J. J.; Brothers, E.; Kudin, K. N.; Staroverov, V. N.; Kobayashi, R.; Normand, J.; Raghavachari, K.; Rendell, A.; Burant, J. C.; Iyengar, S. S.; Tomasi, J.; Cossi, M.; Rega, N.; Millam, N. J.; Klene, M.; Knox, J. E.; Cross, J. B.; Bakken, V.; Adamo, C.; Jaramillo, J.; Gomperts, R.; Stratmann, R. E.; Yazyev, O.; Austin, A. J.; Cammi, R.; Pomelli, C.; Ochterski, J. W.; Martin, R. L.; Morokuma, K.; Zakrzewski, V. G.; Voth, G. A.; Salvador, P.; Dannenberg, J. J.; Dapprich,

S.; Daniels, A. D.; Farkas, Ö.; Foresman, J. B.; Ortiz, J. V.; Cioslowski, J.; Fox, D. J. Gaussian, Inc., Wallingford CT, 2010.